Prion-Protein-Specific Aptamer Reduces PrP^{Sc} Formation

Daniela Proske,[a, d]+ Sabine Gilch,[b]+ Franziska Wopfner,[b] Hermann M. Schätzl,[b] Ernst-L. Winnacker,[a] and Michael Famulok*[a, c]

The critical initial event in the pathophysiology of transmissible spongiform encephalopathies (TSEs) appears to be the conversion of the cellular prion protein (PrP^C) into the abnormal isoform PrP^{Sc}. This isoform forms high-molecular-weight protease K (PK) resistant aggregates that accumulate in the central nervous system of affected individuals. We have selected nuclease-resistant 2′-amino-2′-deoxypyrimidine-modified RNA aptamers which recognize a peptide comprising amino acid residues 90 – 129 of the human prion protein with high specificity. This domain of prion proteins is thought to be functionally important for the conversion of PrP^C into its pathogenic isoform PrP^{Sc} and is highly homologous among prion proteins of various species including mouse, hamster, and man. Consequently, aptamer DP7 binds to the full-length human, mouse, and hamster prion protein. At low concentrations in the growth medium of persistently prion-infected neuroblastoma cells, aptamer DP7 significantly reduced the relative proportion of de novo synthesized PK-resistant PrP^{Sc} within only 16 h. These findings may open the door towards a rational development of a new class of drugs for the therapy or prophylaxis of prion diseases.

KEYWORDS:

aptamers · molecular evolution · prion protein · prion therapy · RNA recognition

Introduction

The conversion of the normal cellular prion protein (PrP^C) into its abnormal isoform PrP^{Sc} is thought to be associated with the pathogenesis of transmissible spongiform encephalopathies (TSEs). The transformation of PrP^C to PrP^{Sc} goes along with a posttranslational structural change from an α-helix/random-coil to a β-sheet conformation.[1–4] This conformational change requires the presence of exogenous or endogenous PrP^{Sc}, a highly infectious proteinaceous particle. Pathologically, the properties of infectious prion proteins ultimately lead to neuronal cell death, vacuolation, and eventually the formation of fibrillous plaques in the central nervous system of affected individuals, resulting in an irreversible spongiform degeneration of brain tissue.

Although the details of the mechanism of prion propagation have remained largely obscure, there are currently two popular hypotheses of how infectious PrP^{Sc} is formed in vivo. According to the protein-only hypothesis, PrP^{Sc} forms a heterodimer with PrP^C which leads to PrP^{Sc}-dependent conversion of PrP^C and subsequent fast formation of a PrP^{Sc}-homodimer.[2, 5] In an autocatalytic process, the formation of additional heterodimers can be exponentially accelerated. Despite intensive efforts, the unambiguous proof of the existence of PrP heterodimers is still missing.[6, 7] The second possible mechanistic model of prion propagation is the nucleation-dependent polymerization model which is based on the assumption that PrP^{Sc} acts as a crystal seed at the starting point for crystal-like growth of a PrP^{Sc} oligomer.[8] This model differs from the previous one in that the infectious particle is formed by a PrP^{Sc} oligomer that can act as the seed for the subsequent polymerization to a high-molecular-weight polymer. Endogenous PrP^C spontaneously and reversibly transforms into a conformation resembling a PrP^{Sc}-like transition state in a fast thermodynamic equilibrium. In the rate-limiting step, PrP in this conformation is deposited onto the crystal seed, which dictates its conformation to the transition state. The changes in secondary and tertiary structure are accompanied by a significantly reduced solubility of PrP in nonionic detergents and dramatically enhanced partial resistance against digestions with proteinase K, which may be a consequence of the formation of high-molecular-weight aggregates.[9] The self-propagating activity of PrP^{Sc} is supported in part by experiments in cell-free in vitro conversion systems,[10] but it still remains to be shown that

[a] *Prof. Dr. M. Famulok, Dr. D. Proske,+ Prof. Dr. E.-L. Winnacker*
Institut für Biochemie, Genzentrum der LMU München
Feodor-Lynen-Strasse 25, 81377 München (Germany)
Fax: (+49) 228-735388
E-mail: m.famulok@uni-bonn.de

[b] *S. Gilch,+ Dr. F. Wopfner, Prof. Dr. H. M. Schätzl*
Max von Pettenkofer-Institut für Virologie
Genzentrum der LMU München
Feodor-Lynen-Strasse 25, 81377 München (Germany)

[c] *Prof. Dr. M. Famulok*
Kekulé Institut für Organische Chemie und Biochemie
Gerhard-Domagk-Strasse 1, 53121 Bonn (Germany)

[d] *Dr. D. Proske+*
Present address:
NascaCell GmbH, Bahnhofstrasse 9 – 15
82327 Tutzing (Germany).

[+] *These authors contributed equally to this work.*

PrP^{Sc} formed in vitro is infectious in vivo. Furthermore, a certain amount of input PrP^{Sc} has so far yielded only stoichiometric amounts of converted PrP^{Sc}; continuous formation of PrP^{Sc} has not yet been observed in cell-free conversion systems, although it was recently shown that sulfated glucosaminoglycans such as Pentosan polysulfate can act as stimulating factors in conversion experiments in vitro.[11]

Whether other factors (for example, factor X[12, 13]) are required for this process in addition to PrP^{Sc} and PrP^{C} still remains controversial. Interestingly, several agents have been found to be capable of negatively affecting the conversion of PrP^{C} into PrP^{Sc}.[14] Many of these compounds belong to the group of polysulfonated, polyanionic drugs (for example, Congo Red, Pentosan polysufate, Dextran sulfates). Other compounds are derivatives of polyene antibiotics or anthracycline. Recent examples are synthetic peptides,[15, 16] porphyrin compounds,[17] soluble lymphotoxin beta receptor,[18] quinacrine, chlorpromazine,[19] and Suramin.[20] Most of these compounds are highly toxic in vivo and are not able to efficiently cross the blood – brain barrier. Very recently, anti-PrP antibodies have been shown to interfere with PrP^{Sc} biogenesis.[21–23]

Based on these very promising studies, we sought to investigate an alternative approach for obtaining novel classes of reagents that may affect the generation of PrP^{Sc} by binding to surface PrP^{C}. We have used in vitro selection of combinatorial nucleic acid libraries to isolate nucleic acid aptamers which specifically bind PrP^{C}. Aptamers have been established as potent tools in molecular biology and diagnostics.[24–28] The spectrum of 'antigens' recognized by nucleic acid ligands and the binding characteristics for their 'epitopes' are in many aspects equivalent to those of monoclonal antibodies or scFv. In most cases, aptamers have also been shown to modulate the biological function of their targets in a highly specific manner. This was demonstrated for a large number of aptamers mostly directed against extracellular target proteins;[24] in a few cases, the biological function of intracellular targets was modulated.[29-33] Previously, we have described an aptamer that recognized prions in brain homogenates of various species including hamster, mouse, and man.[34] The goal of the present work was to: 1) obtain aptamer sequences which bind to a domain of PrP thought to be implicated in prion conversion, 2) demonstrate their resistance against nuclease degradation allowing their application in cell culture systems and, at a later stage, in infected animals, and, 3) also affect the de novo formation of PrP^{Sc} in a cell culture by using a persistently PrP^{Sc}-producing neuronal cell line.

Results and Discussion

As a target peptide for the aptamer selection we chose the domain of the human prion protein comprising amino acid residues (aa) 90 – 129. This peptide sequence was chosen because it belongs to a short epitope (aa 90 – 141) that, on the basis of several lines of evidence, is functionally important for the conversion of PrP^{C} into PrP^{Sc}.[15, 35, 36] For example, it was shown that aa 109 – 122, especially the hydrophobic sequence AGAAAGA, exhibited a high tendency for self-aggregation.[37] Peretz et al. demonstrated that residues 90 – 120 are accessible in PrP^{C}, but not in the PK-resistant fragment $PrP^{27–30}$.[35] Denaturation of $PrP^{27–30}$ exposed the epitopes of the N-terminal domain, which was taken as an indication that the major conformational change underlying PrP^{Sc} formation occurs within the N-terminal segment of $PrP^{27–30}$. In accordance with these findings, no defined secondary structure could be assigned for this region (aa 90 – 127) in NMR spectroscopy structural elucidations of the prion protein of various species.[3, 38–43] Furthermore, a minimal prion protein of 106 amino acids in which aa 23 – 88 and aa 141 – 176 were deleted revealed the typical symptoms of prion infection and prion propagation when transgenic knock-in mice ($Tg(PrP106)Prnp^{0/0}$) were infected with prions.[36]

Three major sequence families dominate the selected anti-prion aptamers

We therefore used peptide 90 – 129 from human PrP as a target for the in vitro selection of high-affinity-binding 2′-aminopyrimidine-modified RNA aptamers from a library of approximately 10^{15} different sequences. This domain is highlighted in the three-dimensional structure shown in Figure 1 A.

The peptide was immobilized on thiopropyl sepharose through a disulfide-bond formed with an N-terminal additional cysteine residue (Figure 1 B). The in vitro selection was performed with an RNA pool which bore primer binding sites optimized for T7-transcription by using 2′-amino-2′-deoxypyrimidine triphosphates. When the resulting modified RNA pool was incubated with 10% fetal calf or human blood serum, no significant RNase degradation could be observed within 24 h (data not shown), which is in accordance with observations from other laboratories.[44, 45] A preselection with the nonderivatized matrix was included in each selection cycle. The stringency of the selection was gradually increased in subsequent cycles by reducing the concentration of immobilized peptide on the matrix ranging from $\sim$40 μM in the first three cycles to 1.4 μM in the final two cycles. After 12 cycles of iterative selection and amplification, the binding pool was cloned into the vector pGEM 4Z, and 43 clones were sequenced. The sequences obtained could be grouped into three different sequence families (Figure 2 A).

Family I is represented by a single predominating sequence and mutants thereof; this family makes up to 77% of the selected pool. Family II is represented by 14%, and family III by 7% of all clones sequenced. In addition, one orphan sequence (clone DP27) was identified. Members within each family differ only by point mutations, deletions, or insertions. No sequence homologies were identifiable among the three families.

The proposed secondary structure of the most abundant aptamer DP7 is shown in Figure 2 B. The presence of several repetitive guanosine residues suggests that DP7 and the mutants comprising motif I form a G-quartet secondary structure motif. This is supported by the following lines of evidence: first, computer-generated foldings[46] indicated that DP7 has a remarkably poor ability to form helices and, hence, stable secondary structures other than G quartets; second, Figure 2 A reveals a high degree of variation among the motif I family

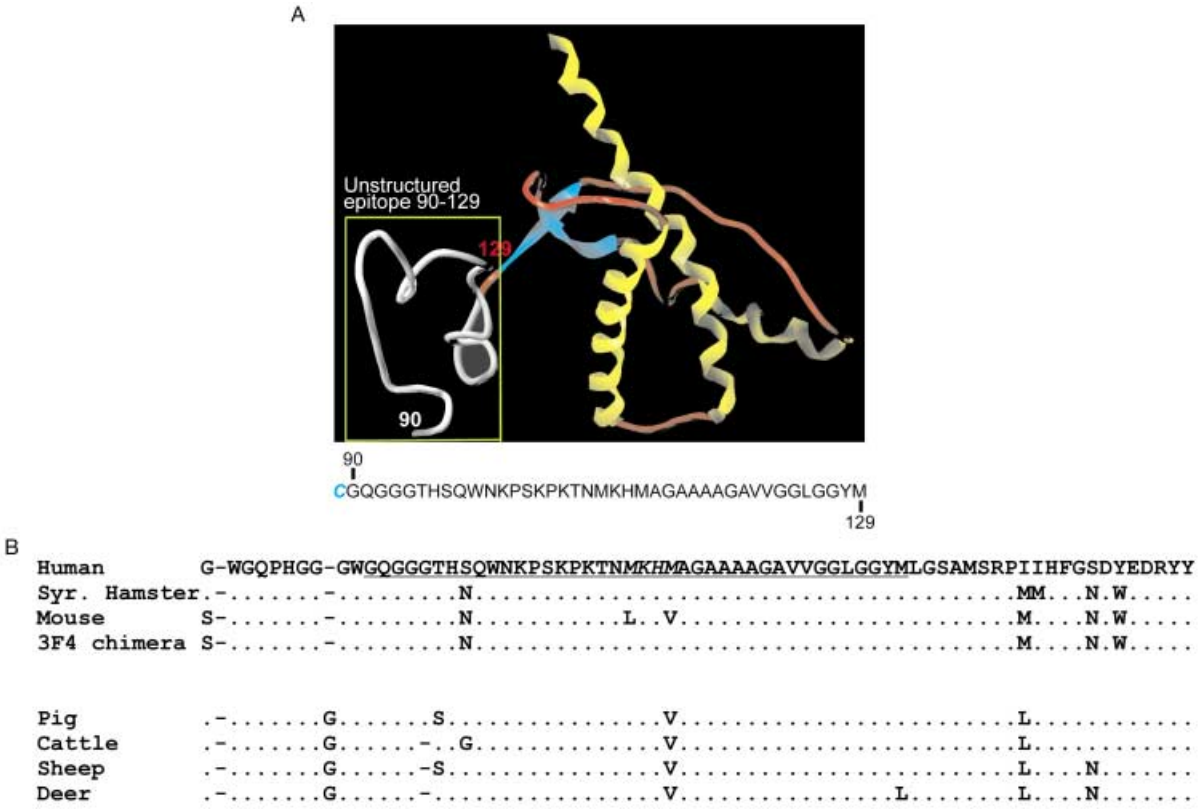

Figure 1. *A) Location of the epitope 90 – 129 (box) in the three-dimensional structure of the human prion protein. The epitope is located at the surface of the protein and exhibits no defined conformation. The sequence of the epitope is shown below the structure. The cysteine residue shown in cyan was added to allow immobilization of the peptide epitope on thiopropyl sepharose. B) Amino acid sequence alignment of mouse, hamster, and human PrP and the 3F4 PrP chimera. In the chimeric mouse – hamster – mouse (3F4) PrP amino acid residues 94 – 131 of murine full-length PrP were replaced by the corresponding hamster sequence. The human PrP peptide epitope 90 – 129 is underlined in the human PrP sequence. Sequence homologies in this region are high, as shown by the related epitopes of PrP from species not investigated here, namely pig, cattle, sheep, and deer.*

between aa 30 – 44. Exactly these residues comprise a large loop region in the proposed G-quartet secondary structure. The variations in clones 16 and 20 (G34U) and a variation in clone 5 (G37U) provide strong evidence that G33G34 and G36G37 are not engaged in G-quartet formation. In a previous study, an in vitro selection of an unmodified RNA library against recombinant Syrian hamster PrP led to the isolation of RNA aptamers with G-quartet structure that bound to the N terminus (aa 23 – 52) of the protein.[34] These aptamers significantly differed in their primary sequence from those isolated here and do not share any similarities despite the potential ability to form G-tetrad structures.

Aptamers bind to the full-length recombinant prion protein

The goal of this study was to investigate whether selected aptamers can affect the conversion of PrP^{c} into PrP^{Sc}. Therefore, we had to ensure that the peptide-binding aptamer motifs are also capable of recognizing the full-length proteins. The binding affinities of individual clones from each aptamer sequence family were determined by filter-binding assays with recombinant full-length PrP from Syrian hamster. The recombinant hamster full-length protein was titrated with radiolabeled aptamer RNAs at increasing protein concentrations ranging from 1 nM to 10 μM. The binding assay contained heparin as an unspecific competitor. RNA/protein complexes were separated from unbound molecules by nitrocellulose filtration, and retained RNA was quantified by phosphorimaging. Dissociation constants (K_d values) were determined from the resulting binding curves as summarized in the legend of Figure 2.

The unselected pool was used as a negative control. No binding of the unselected pool RNA to hamster PrP was detected at the maximum concentration at which the protein remained in solution in the presence of RNA. The maximum PrP concentration that could be used in the filter-binding assay was 10 μM due to precipitation of the protein at higher concentrations even in the presence of various detergents. The most abundant sequence (DP7) recognizes prion protein from Syrian hamster with a dissociation constant of 100 nM as summarized in the legend of Figure 2. Members from other sequence families bind with significantly lower affinities. We therefore chose to characterize DP7 in more detail.

First, we were interested in whether DP7 was able to recognize prion proteins from various species. Human and hamster PrP are highly homologous; within the region of aa 90 – 129 (Figure 1 B) they differ only by one amino acid exchange.[47] Therefore, the binding affinity of DP7 to hamster PrP was compared with that of the mouse, and human full-length recombinant PrPs. In addition, a chimeric mouse – hamster –

A

Clone	Sequence	K_d (μM)
Motif I		
7 (25)	GTGCTATGGA-GTGGAGGAGTTGAAGGTGTCGGGGTTGGC	0.1
1 (2)	.....A.....	
5	.....T....-.....	
14	.....C.....	
16	.....T.....C.....-.....	
20	.....T.....	
21	.....A.....	
23	.....-.....	
Motif II		
2 (2)	TAGGAGGAGGTGTGAAGGTGGGGTAGGATAGGAAGTTAACC	10
11 (3)	.....-..	
35	.....-.....	
Motif III		
6	TCCCAAGGTGGGGCGTAGAGGGGAGATGCGGTGCG--CTGA	3
38	.....GC....	
22	...-.....	
Orphan		
27	ATAGAGTCCGGAAAGGGTACAGCGGAGGCTGGGTGTGGAGG	7
(Pool)	NNNNNNNNNNNNNNNNNNNNNNNNNNNNNNNNNNNNNNNN	no affinity

B

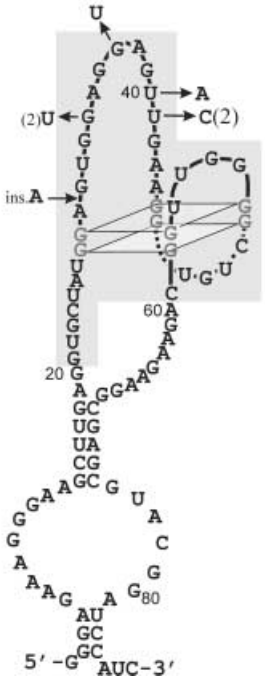

Figure 2. *A) Sequences and abundance of the clones from the prion peptide selection. Only the randomized region is shown for each clone. The number of multiply isolated clones is given in parentheses after each clone number. The 2′-amino-2′-deoxycytidine or -thymidine residues are abbreviated C and T, respectively. Mutations and deletions (–) within each family are shown. All pyrimidine residues were 2′-deoxy-2′-amino derivatives. Residues proposed to form a G-tetrad structure are shown in the gray boxes. Dissociation constants (K_d) of Syrian hamster PrP with individual aptamer sequences from different sequence families are also shown. K_ds were determined from the binding kinetics by using Equation (1) where* Q *is the fraction of equilibrium-bound RNA,* P_t *and* R_t *the total peptide and RNA concentrations,* and f *is the efficiency of complexes retained on nitrocellulose:*[58]

$$Q = (f/2R_t) = (P_t + R_t + K_d) - [(P_t + R_t + K_d)^2 - 4P_tR_t]^{1/2} \quad (1)$$

mouse (3F4) PrP was used in which aa 94 – 131 of murine full-length PrP were replaced by the corresponding hamster sequence.[48] Figure 3 A shows the titration curves of these

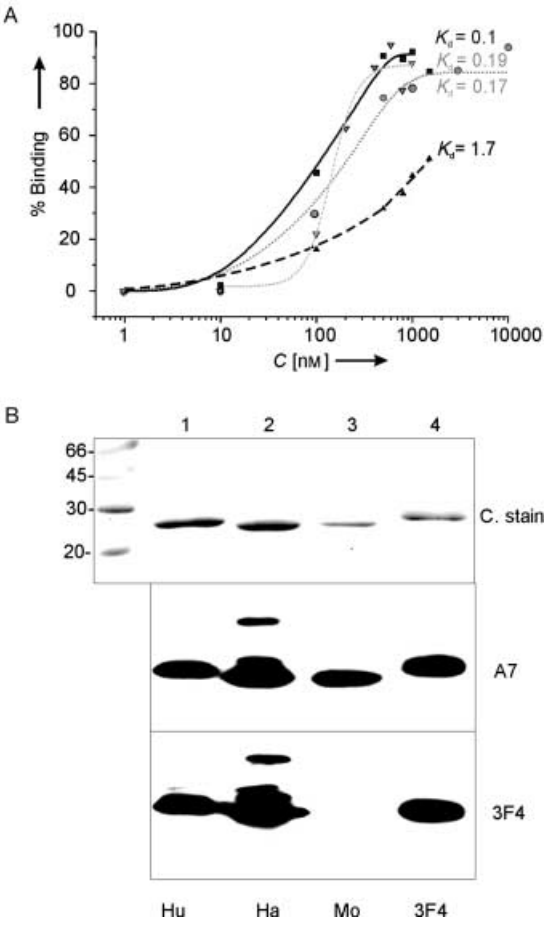

Figure 3. *Binding of DP7 to* PrP^C *from various species. A) Filter-binding studies of full-length prion proteins from various species. Reactions (50 μL) containing 0 – 10 μM protein, 5′-*^{32}*P-labeled aptamer DP7, in assay buffer were incubated, then filtered through prewashed 0.45 μM nitrocellulose membranes, and washed five times with phosphate-buffered saline (PBS; 5.0 mL). RNA remaining on the filter was quantified on a standard PhosphoImager. ■, mouse PrP; ●, Syrian hamster PrP; ▲, human PrP; ▼, mouse – hamster – mouse chimera 3F4. The* K_d*s for DP7-binding are shown for each of the different PrPs. B) Analysis of full-length prion proteins from various species. Recombinant prion proteins from human (Hu), Syrian hamster (Ha), mouse (Mo), and the mouse – hamster – mouse chimera (3F4) were analyzed by SDS-PAGE followed by Coomassie Blue staining (upper panel). Molecular size markers are indicated on the left. The middle and lower panels show an immunoblot analysis of the identical proteins, by using either a polyclonal anti-PrP antibody (A7) or the monoclonal anti-PrP antibody 3F4. Monoclonal antibody 3F4 reacts against human, Syrian hamster, and 3F4-tagged chimeric PrP, but not against murine PrP (lower panel/lane 3).*

experiments and summarizes the K_d values calculated from these titrations; the values were determined in the same way as described in the legend of Figure 2. The integrity of recombinant proteins was analyzed by SDS-PAGE combined with Coomassie Blue staining and by immunoblot analysis with monoclonal and polyclonal anti-PrP antibodies as described elsewhere (Figure 3 B).[20]

Interestingly, while the epitope 90 – 129 from human PrP was used as the selection target, DP7 turned out to bind human full-length PrP under our experimental conditions with approximately tenfold lower affinity than the full-length murine or hamster PrPs. At present we do not have an explanation for

these observed differences. These data show that it is possible to select aptamers with affinity to an accessible peptide epitope that are also capable of recognizing the complete prion protein. In previous studies, Xu and Ellington selected an aptamer that bound to an epitope of the Rev protein from human immunodeficiency virus I (HIV-1).[49] Just as antibodies that recognize peptide epitopes can often recognize the corresponding epitope when presented in a protein, the Rev peptide-binding aptamers were found to specifically bind to the full-length Rev protein. Another example is aptamers selected to bind epitopes from $\alpha_L\beta_2$-integrin.[31]

DP7 reduces PrP^{Sc} formation in persistently prion-infected neuroblastoma cells

To investigate whether the presence of DP7 in the cell culture medium affects the de novo generation of PrP^{Sc} aggregates we used a persistently prion-infected murine neuroblastoma cell line (3F4-ScN2a). These cells stably express a chimeric mouse – hamster – mouse (MHM2) PrP in addition to endogenous mouse PrP.[48] The hamster sequence (aa 94 – 131) provided the epitope for the monoclonal anti-PrP antibody 3F4 (aa 109 – 112) used for the selective immunoprecipitation of de novo generated PrP^{Sc}. Our strategy was to quantify metabolically labeled PrP^{Sc} resulting from cells cultured in the presence of low concentrations of the aptamer.

Negative control experiments were performed in parallel by employing untreated cells and addition of an unselected RNA library, respectively. Each experiment was repeated at least six times, that is, two independent experiments were each measured in triplicate, to obtain statistically relevant evidence. Aptamer DP7 and pool RNA remained stable under these conditions (data not shown).

The experimental set-up is shown schematically in Figure 4 A. After 16 h of radioactive labeling of de novo synthesized PrP^{Sc} with ^{35}S-methionine/cysteine in the presence of 700 nM RNA aptamer, the cells were lyzed, and halves of the postnuclear supernatants were separately ultracentrifuged. One half was treated with proteinase K before ultracentrifugation. The ultracentrifugation in the presence of 1% sarcosyl ensures sedimentation of PrP^{Sc} while PrP^{c} remains dissolved in the supernatant. PrP^{Sc} from the pellet samples was redissolved and immunoprecipitated with the mAb 3F4. The amount of total de novo generated, insoluble PrP can be obtained by quantifying samples without PK treatment (Figure 4 B, lanes 1 – 9), whereas the PK-treated samples shown in Figure 4 B (lanes 10 – 18) reveal both insolubility and resistance to PK digestion. As the mAb 3F4 cannot detect the endogenous murine PrP (see Figure 3 B), the radioactive PrP signal in Figure 4 B can only be due to the chimeric mouse – hamster – mouse 3F4-PrP construct.

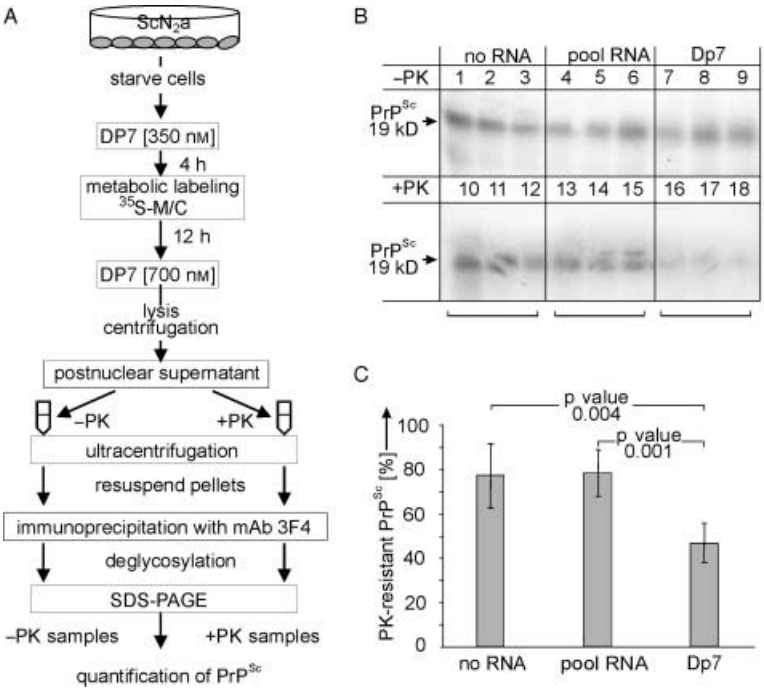

Figure 4. *Aptamer-dependent reduction of the amount of de novo generated PK-resistant PrP^{Sc}. A) Experimental set-up for the analysis of de novo generated PrP^{Sc} in 3F4-ScN2a cells. After 16 h of radioactive labeling with ^{35}S-Met/Cys in the presence of 700 nM aptamer (4 h pretreated with 350 nM) the cells were lyzed, centrifuged, and one half of the postnuclear supernatant was treated with proteinase K (PK; 20 μg mL^{-1} for 30 min), while the other half was not. To separate PrP^{Sc} from PrP^{C}, both samples were ultracentrifuged in the presence of 1% sarcosyl (1 h, 100 000 g). Sedimented PrP^{Sc} was redissolved and immunoprecipitated with the 3F4 antibody. As a maximal conversion of 1 – 5% of the newly translated PrP^{C} into PrP^{Sc} can be expected,[59] the samples were completely deglycosylated with PNGaseF to increase the sensitivity of detection. B) Denaturing PAGE of immunoprecipitated and deglycosylated PrP. Top panel (lanes 1 – 9): triplicate analysis without proteinase K treatment (– PK). Lanes 1 – 3: negative control without RNA; lanes 4 – 6: negative control in presence of 700 nM pool RNA; lanes 7 – 9: experiment in the presence of 700 nM DP7 aptamer. Bottom panel (lanes 10 – 18): triplicate analysis with proteinase K digestion (+ PK). The PrP shown in lanes 10 – 18 represents de novo generated PK-resistant PrP^{Sc}. Lanes 10 – 12: negative control without RNA; lanes 13 – 15: negative control in the presence of 700 nM pool RNA; lanes 16 – 18: experiment in the presence of 700 nM DP7 aptamer. Samples were analysed by 12.5% SDS-PAGE and the ^{35}S-signal was quantified by PhosphorImaging. C) Quantification of the percentage of de novo generated PrP^{Sc} and statistical evaluation of six independent measurements. The columns show the proportion of PK-resistant PrP^{Sc} in relation to total de novo synthesized insoluble PrP. The* p*-values were calculated by using student's* t*-test (*n = 6*).*

Quantification revealed that the absolute amount of de novo synthesized, insoluble PrP is not significantly affected by the presence of the aptamer DP7 (Figure 4 B, lanes 7 – 9) compared to the pool RNA (lanes 4 – 6) or the RNA-free negative control (lanes 1 – 3). However, the relative proportion of PK-resistant PrP^{Sc} material is significantly reduced in the presence of the aptamer DP7 (Figure 4 B, lanes 16 – 18) relative to the negative control without RNA and pool control samples (lanes 10 – 12 and 13 – 15, respectively). The quantification of the total amount of de novo synthesized, insoluble PrP revealed a 53% reduction of the relative proportion of PK-resistant PrP with respect to the non-PK-treated samples in the presence of 700 nM aptamer DP7 (Figure 4 B, lanes 7 – 9 and 16 – 18) within 16 h. Note that the observed 50% reduction is indicative of an IC_{50} value in the nanomolar range in cultured cells.

Statistical analysis of the data showed that the presence of 700 nM DP7 led to a p value (an admeasurement for the quantification of differences between test groups in statistical analyses) of 0.001 relative to the pool RNA negative control, and 0.004 relative to the negative control in the absence of RNA ($n = 6$; Figure 4C). In contrast, the p value of the "pool versus no RNA" negative control experiments was 0.9 and confirmed that the observed reduction of PK-resistant PrP^{Sc} is aptamer-specific and highly reproducible (Figure 4C). The aptamer had no significant effect on the total amount of de novo generated insoluble PrP, indicating that it mainly affects the formation of insoluble PrP to PK-resistant PrP^{Sc} conformers (Figure 4B).

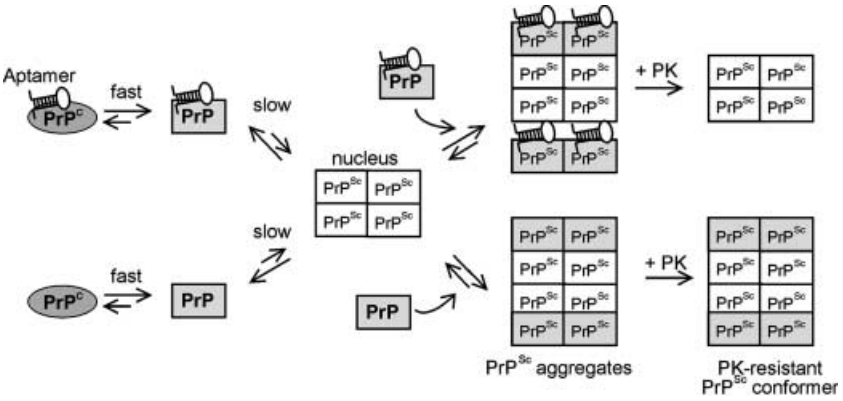

Figure 5. *Model for the mechanism of DP7-specific reduction of PrP^{Sc} formation based on the nucleation-dependent polymerization model as proposed by Lansbury and Caughey.[8] Aptamer DP7 binds initially to surface-located PrP^{c} and remains bound to PrP. The de novo formation of high-molecular-weight tightly folded PrP^{Sc} aggregates originating on a preexisting crystal seed is modulated in the presence of the aptamer. The acquisition of proteinase K resistance is directly connected with aggregate formation and tight folding. In the presence of the aptamer binding to PrP, PK-resistance is reduced as a function of diminished formation of the most tightly folded PrP aggregates.*

PrP^{Sc} reduction by aptamer DP7 in light of the nucleation-dependent polymerization model

How does the aptamer DP7 specific reduction of PK-resistant PrP^{Sc} aggregates fit into the various hypotheses describing prion propagation? From a kinetic point of view in the context of the heterodimer model, the initial step of the PrP^{C} into PrP^{Sc} conversion is the binding of PrP^{c} to PrP^{Sc} and the subsequent formation of aggregates which leads to protease resistance of the newly formed PrP^{Sc} complex.[50] For our selected aptamers, which obviously bind initially to surface-located PrP^{c}, no measurable effect on the biogenesis of insoluble PrP was detectable. Instead, only the formation of de novo generated proteinase K resistant PrP^{Sc} conformers is reduced by the aptamer DP7. These experimental observations fit into a model in which the aptamer exhibits an inhibitory effect on the polymerization of PrP^{Sc} molecules to high-molecular-weight and tightly folded aggregates, which is reflected in the reduced PK resistance of the de novo formed PrP^{Sc} material in the presence of DP7. Thereby, it may be possible that in the presence of the aptamer, the quaternary β-sheet structure of the PrP^{Sc} aggregate is altered by the aptamer in such a way that degradation of the less tightly folded PrP aggregates by PK is favored. Notably, our findings are in accordance with previous studies in which the existence of PrP^{Sc} conformers with different biochemical properties (that is, insolubility combined with sensitivity to PK) was demonstrated.[9] In these studies, the tight folding of PrP^{Sc} conformers was correlated with resistance to PK digestion.[9] Another model would describe a more indirect effect of specific aptamer binding to PrP on PrP^{Sc} formation: it has been suggested that endogenous glycosaminoglycans are required for the formation of PrP amyloids in natural TSE- and scrapie-infected mice.[51, 52] Due to their 2′-amino-2′-deoxy-modified riboses, the aptamers may be structurally related to endogenous glycosaminoglycans. Thereby, it may be possible that the specific binding of the aptamers to PrP competitively reduces the binding of endogenous glycosaminoglycans.[8] Taken together, the models we propose for describing the effect of the aptamer would be consistent with a polymerization model, as illustrated in Figure 5.

During the pathogenesis of spongiform encephalopathies the formation of PrP^{Sc} aggregates (amyloids) and the associated proteinase K resistance correlate with infectivity and neurodegeneration.[53] It was experimentally demonstrated that potential TSE therapeutic compounds such as Dextrane sulfate or Congo Red reduce PrP^{Sc} accumulation in persistently prion-infected neuroblastoma cells. These compounds can also lead to prolonged survival of mice that underwent PrP^{Sc} inoculation after prophylactic treatment with these compounds.[11, 54] However, this effect was only observed if the compounds were administered at peripheral routes around the time of prion infection.[55] Relative to compounds such as these, aptamer DP7 exerts its effect at a low concentration and during a very short period of treatment. It will be interesting to investigate the effect of DP7 in animal models. The potential side effects of anti-prion RNA aptamers, their bioavailability, and their potential to cross the blood – brain barrier can only be studied with in vivo models. Noticeably, our recent studies with the compound Suramin and with anti-PrP antibodies have pointed to a similar and eventually more general molecular mechanism in which molecules interfere with prion propagation by interfering with PrP^{c} surface expression.[20] RNA aptamers which can be selected for a high binding affinity to surface-located PrP^{c} might represent an ideal example of this class of anti-prion compounds.

Conclusion

The anti-prion RNA aptamer DP7 acts at very low concentrations and within a short time relative to other agents known to reduce the accumulation of the protease-resistant isoform of PrP, namely sulphated glycans, polyene antibiotics, Congo Red, anthracycline, porphyrins, chlorpromazine, quinacrine, and Suramin.[14] Furthermore, by using an overlapping series of synthetic peptides covering the amino acid sequence of PrP, it was shown

that peptides encompassing amino acid residues 109 – 141 led to species-independent reduction of PrP^{Sc} accumulation in an in vitro conversion assay.[16] While these results supported a role of this region in the conversion process, it is unclear whether the peptides acted as ligands for PrP. Here, we have shown for the first time that selective targeting of a presumed functional domain of PrP by a specific synthetic nucleic acid binder DP7 results in the reduction of PrP^{Sc} accumulation in prion-infected cells.

Fortunately, despite the alarming cases of new varient Creutzfeldt – Jakob disease (nvCJD) in the United Kingdom, TSEs in humans still can be considered a fairly rare disease from an epidemiological point of view. It is difficult to foresee how the incidence of nvCJD will develop, because of a likely long incubation time. Clearly, molecular tools are needed that allow us to illuminate mechanisms of the pathogenesis of TSEs, which will help investigations into novel ways of therapy or prophylaxis. Aptamer DP7 should be useful for studying molecular mechanisms of prion propagation in cells and model organisms. More importantly, DP7 could represent the first of a novel class of designed agents for a rational therapeutic or prophylactic approach against TSEs.

Experimental Section

Materials: All solutions were made in baked glassware to minimize ribonuclease contamination. Buffers and salt solutions were prepared from filtered and deionized water and then filter-sterilized through 0.45 μm membranes (Millipore) or autoclaved. Enzymes and chemicals were from the following manufacturers: AMV reverse transcriptase, RNAsin (Promega); alkaline phosphatase CIP, restriction endonucleases, T4 DNA ligase, T4 RNA ligase, and polynucleotide kinase (NEB); Taq-polymerase, Tth-polymerase, dNTPs, and NTPs (Boehringer-Roche); ^{32}P-labeled NTPs, dNTPs, and ^{35}S-methionine/cysteine (NEN and Amersham-Pharmacia); T7 RNA polymerase (Stratagene). 2′-Amino-2′-deoxy-UTP and -CTP were synthesized as described[56, 57] and kindly provided by O. Thum, Kekulé-Institut für Organische Chemie and Biochemie, University of Bonn, Germany. The monoclonal anti-PrP antibody 3F4 was from Signet Laboratories (Dedham, MA, USA). The polyclonal anti-PrP antibody A7 has been described elsewhere.[20a] DNA oligonucleotides and primers were synthesized on a Millipore Expedite oligonucleotide synthesizer by using solid-phase phosphoramidite chemistry or purchased in HPLC-purified form from Metabion (Munich) and MWG (Ebersberg). Sequences for the construction of the modified RNA library were 5′-GGGAGAAAGGGAAGCTTGAG-40N-AGAAGAAGGACGAGCGTACG-GATCCGATC-3′ (Mod40N). Sequences for the primers used for amplification of these oligonucleotides were 5′-TCTAATACGACT-CACTATAGGGAGAAAGGGAAGCTTGAG-3′ (PM39 – 5′) and 5′-CTTCCTGCTCGCATGCCTAGGCTAG-3′ (PM25 – 3′).

Recombinant prion proteins: Recombinant PrPs of murine, Syrian hamster, and human origin, as well as a 3F4-tagged version of murine PrP, were constructed. For *E. coli* expression and purification, we sub-cloned PrP constructs not containing the N- and C-terminal signal peptides into the bacterial expression vector pQE30, thereby providing an N-terminal polyhistidine tag. Expression was done in proteinase-deficient bacteria (strain BL21). Four hours after induction with 2 mM isopropyl-β-D-thiogalactopyranoside (IPTG), bacteria were lyzed in 6 M guanidium hydrochloride buffer (6 M guanidium hydrochloride, 20 mM sodium phosphate, 500 mM sodium chloride, pH 7.8), cellular debris was removed by centrifugation at 10 000 g for 20 min, and the soluble fraction was loaded onto a Ni^{2+} column (ProBond, Invitrogen) pre-equilibrated with binding buffer (8 M urea, 20 mM sodium phosphate, 500 mM sodium chloride, pH 7.8). The column was washed several times (8 M urea, 20 mM sodium phosphate, 500 mM sodium chloride, 80 mM imidazole, pH 6.3), and the His-tagged fusion protein was eluted (8 M urea, 20 mM sodium phosphate, 500 mM sodium chloride, 500 mM imidazole, pH 6.3). Eluted fractions (0.5 mL) with the highest protein concentrations were pooled, urea was removed, and PrP was refolded by dialysis against ultrafiltrated water. Untagged full-length murine and Syrian hamster recombinant PrP (aa 23 – 231) were obtained from Prionics (Zürich, Switzerland). Integrity of recombinant proteins was analyzed by SDS-PAGE combined with Coomassie Blue staining and by immunoblot analysis with monoclonal and polyclonal anti-PrP antibodies as described elsewhere.[20a]

Immobilization of the PrP peptide (aa 90 – 129) on thiopropyl sepharose: Sepharose 4B (500 mg, Pharmacia) was swollen and equilibrated in coupling buffer (3.5 mL) washed according to the manufacturer's instructions. The coupling of various amounts of peptides proceeded overnight at 4 °C. As a negative control, one Sepharose sample (500 mg) was treated in the same way but without peptide. The amount of immobilized material was determined by spectroscopic quantification of thiopyridone that was released during the coupling ($\lambda = 343$ nm; $\varepsilon = 7060\,\mathrm{M^{-1}\,cm^{-1}}$). Coupling efficiency was 45 – 60 %. Unreacted 2-thiopyridyl residues were blocked by reaction with 5 mM 2-mercaptoethanol in NaOAc (100 mM, pH 6.0). After washing with NaOAc (100 mM, pH 6.0), the matrix was stored in binding buffer at 4 °C for a maximum of 2 weeks without measurable degradation.

In vitro selection: The radiolabeled RNA library was denatured at 90 °C in Mg^{2+}-free selection buffer (155 mM NaCl, 1.1 mM KH_2PO_4, 3.0 mM Na_2HPO_4, 1.0 mM $MgCl_2$, pH 7.4) prior to each selection cycle. The RNA was preselected on underivatized Sepharose or on Sepharose that was derivatized with unrelated peptides, before incubation with the Sepharose derivatized with the target peptide sequence. The preselected RNA (13 μM in cycle 1, 13.3 μM in subsequent cycles) was incubated with target – Sepharose at 37 °C for 1 h in a thermo-mixer. Samples were transferred onto a chromatography column, and nonbinding RNAs were removed by intensive washes with binding buffer (100 column volumes). Bound RNAs were eluted with sodium dodecylsulfate (SDS) buffer (1.0 mL; 0.5 M tris(hydroxymethyl)aminomethane – HCl (Tris-HCl; pH 7.6), 3.2 mL glycerol, 6.4 mL, 5 % SDS, 3.2 g 1,4-dithiothreitol (DTT), 4.6 mL water), or reductively cleaved off from the matrix from cycle 9 onwards. The eluted RNA was extracted with phenol/$CHCl_3$ (2 ×), precipitated with ethanol, washed twice with 70 % EtOH, redissolved in water, reverse transcribed, PCR amplified, and in vitro transcribed as described previously.

RNA/protein binding assay: 5′-^{32}P-labeled RNA aptamers were denatured for 3 min at 85 °C in 0.5 × phosphate-buffered saline (PBS), at pH 7.4 without $CaCl_2$ and $MgCl_2$ (Gibco), supplemented with 2 mM $MgCl_2$, and placed on ice for refolding for 15 min. Purified recombinant proteins were equilibrated to 0.16 × PBS and centrifuged at 100 000 g in a TL-100 ultracentrifuge (Beckmann) for 1 h at 4 °C to remove insoluble protein aggregates. Increasing amounts of soluble proteins (for Syrian hamster PrP 0 – 10 μM, mouse PrP 0 – 3 μM, 3F4-mouse PrP 0 – 1 μM, and human PrP 0 – 1.5 μM) were incubated with RNA (1.5 nM), Na – heparin (3 $\mu g\,\mu L^{-1}$; Sigma) and 0.16 × PBS in a total volume of 50 μL for 1 h at 37 °C with weak shaking (7000 rpm). Samples were passed through 0.45 μm nitrocellulose filters (Millipore), and unbound RNA aptamers were removed by washing with

1 × PBS (5 mL). The percentage of bound RNA was calculated after PhopholmagerTM quantification in relation to the corresponding amount of RNA used in the assay.

Analysis of de novo synthesized PrP^{Sc} from prion-infected neuroblastoma cells: Persistently prion-infected murine neuroblastoma cells overexpressing a 3F4-tagged murine PrP (3F4-ScN2a) were passaged 2 d prior to their use and grown in 6 cm petri dishes to 70% confluency. Cells were washed twice with PBS and incubated for 30 min at 37 °C in RPMI-1640 medium containing 1% fetal calf serum (FCS) which was free of methionine and cysteine. De- and renatured RNA in binding buffer was added to this growth medium to a final concentration of 350 nM. After 45 min of incubation, 800 μCi ^{35}S-methionine/cysteine (Amersham) and FCS to a final concentration of 3% were added. After 4 h, the aptamer concentration in the growth medium was adjusted to 700 nM. After incubation for 12 h, cells were washed twice in ice-cold PBS and lyzed in cold lysis buffer (1 mL; 100 mM NaCl, 10 mM Tris-HCl, pH 7.8, 10 mM ethylenediaminetetraacetate (EDTA), 0.5% Triton X-100; 0.5% sodium deoxycholate (DOC)); insoluble material was removed by centrifugation, and the post-nuclear supernatant was divided into two 500-μL samples. One half was subjected to digestion for 30 min with proteinase K (20 μg mL^{-1}). Lysates (± PK) were subjected to ultracentrifugation (1 h at 100 000 g, 4 °C; Beckman TL-100 table ultracentrifuge; TLA-45 rotor) in the presence of 1% sarcosyl. Pellets were resuspended in radioimmunoprecipitation assay (RIPA) buffer (100 μL; 0.5% Triton X-100, 0.5% DOC, in PBS) with 1% SDS, boiled for 10 min, and diluted with 900 μL RIPA buffer (supplemented with 1% sarcosyl). The primary antibody (3F4) was incubated overnight at 4 °C. Protein A Sepharose beads were then added for 90 min at 4 °C. The immunoadsorbed proteins were washed in RIPA buffer supplemented with 1% SDS, subjected to a deglycosylation step with PNGaseF, and analyzed by 12.5% SDS-PAGE followed by autoradiography. The ^{35}S signals of the deglycosylated PrP bands were quantified by phosphoimaging.

We thank Michael Blind and Günter Mayer for helpful discussions. This work was supported by grants from the German Bundesministerium für Bildung und Forschung (BMBF) to M.F. and E.-L.W., the Deutsche Forschungsgemeinschaft (Grant: SCHA 594/3 – 3), the EU BIOMED (Grant: CT98 – 6040), and FAIR (Grant: CT98 – 7020) to H.M.S., and the Fonds der Chemischen Industrie to M.F.

[1] A. Aguzzi, M. A. Klein, F. Montrasio, V. Pekarik, S. Brandner, H. Furukawa, P. Kaser, C. Rockl, M. Glatzel, *Ann. NY Acad. Sci.* **2000**, *920*, 140.
[2] F. E. Cohen, K.-M. Pan, Z. Huang, M. Baldwin, R. J. Fletterick, S. B. Prusiner, *Science* **1994**, *264*, 530.
[3] R. Riek, G. Wider, M. Billeter, S. Hornemann, R. Glockshuber, K. Wüthrich, *Proc. Natl. Acad. Sci. USA* **1998**, *95*, 11 667.
[4] R. Glockshuber, *Adv. Protein Chem.* **2001**, *57*, 83.
[5] S. B. Prusiner, *Science* **1991**, *252*, 1515.
[6] R. K. Meyer, A. Lustig, B. Oesch, R. Fatzer, A. Zurbriggen, M. Vandevelde, *J. Biol. Chem.* **2000**, *275*, 38 081.
[7] S. A. Priola, B. Caughey, K. Wehrly, B. Chesebro, *J. Biol. Chem.* **1995**, *270*, 3299.
[8] P. T. Lansbury, Jr., B. Caughey, *Chem. Biol.* **1995**, *2*, 1.
[9] J. Safar, H. Wille, V. Itri, D. Groth, H. Serban, M. Torchia, F. E. Cohen, S. B. Prusiner, *Nature Med.* **1998**, *4*, 1157.
[10] D. A. Kocisko, J. H. Come, S. A. Priola, B. Chesebro, G. J. Raymond, P. T. Lansbury, Jr., B. Caughey, *Nature* **1994**, *370*, 471.
[11] C. Wong, L. W. Xiong, M. Horiuchi, L. Raymond, K. Wehrly, B. Chesebro, B. Caughey, *EMBO J.* **2001**, *20*, 377.
[12] G. C. Telling, M. Scott, K. K. Hsiao, D. Foster, S.-L. Yang, M. Torchia, K. C. L. Sidle, J. Collinge, S. J. DeArmond, S. B. Prusiner, *Proc. Natl. Acad. Sci. USA* **1994**, *91*, 9936.
[13] G. C. Telling, M. Scott, J. Mastrianni, R. Gabizon, M. Torchia, F. E. Cohen, S. J. DeArmond, S. B. Prusiner, *Cell* **1995**, *83*, 79.
[14] M. W. Head, J. W. Ironside, *Trends Microbiol.* **2000**, *8*, 6.
[15] J. Chabry, B. Caughey, B. Chesebro, *J. Biol. Chem.* **1998**, *273*, 13 203.
[16] J. Chabry, S. A. Priola, K. Wehrly, J. Nishio, J. Hope, B. Chesebro, *J. Virol.* **1999**, *73*, 6245.
[17] S. A. Priola, A. Raines, W. S. Caughey, *Science* **2000**, *287*, 1503.
[18] F. Montrasio, R. Frigg, M. Glatzel, M. A. Klein, F. Mackay, A. Aguzzi, C. Weissmann, *Science* **2000**, *288*, 1257.
[19] C. Korth, B. C. May, F. E. Cohen, S. B. Prusiner, *Proc. Natl. Acad. Sci. USA* **2001**, *98*, 9836.
[20] a) S. Gilch, K. F. Winklhofer, M. H. Groschup, M. Nunziante, R. Lucassen, C. Spielhaupter, W. Muranyi, D. Riesner, J. Tatzelt, H. M. Schätzl, *EMBO J.* **2001**, *20*, 3957; b) S. Gilch, H. M. Schätzl, unpublished data.
[21] M. Enari, E. Flechsig, C. Weissmann, *Proc. Natl. Acad. Sci. USA* **2001**, *98*, 9295.
[22] D. Peretz, R. A. Williamson, K. Kaneko, J. Vergara, E. Leclerc, G. Schmitt-Ulms, I. R. Mehlhorn, G. Legname, M. R. Wormald, P. M. Rudd, R. A. Dwek, D. R. Burton, S. B. Prusiner, *Nature* **2001**, *412*, 739.
[23] F. L. Heppner, C. Musahl, I. Arrighi, M. A. Klein, T. Rulicke, B. Oesch, R. M. Zinkernagel, U. Kalinke, A. Aguzzi, *Science* **2001**, *294*, 178.
[24] M. Famulok, G. Mayer, *Curr. Top. Microbiol. Immunol.* **1999**, *243*, 123.
[25] M. Famulok, G. Mayer, M. Blind, *Acc. Chem. Res.* **2000**, *33*, 591.
[26] M. Famulok, M. Blind, G. Mayer, *Chem. Biol.* **2001**, *8*, 931.
[27] D. S. Wilson, J. W. Szostak, *Annu. Rev. Biochem.* **1999**, *68*, 611.
[28] S. E. Osborne, I. Matsumura, A. D. Ellington, *Curr. Opin. Chem. Biol.* **1997**, *1*, 5.
[29] T. L. Symensma, L. Giver, M. Zapp, G. B. Takle, A. D. Ellington, *J. Virol.* **1996**, *70*, 179.
[30] M. Thomas, S. Chédin, C. Carles, M. Riva, M. Famulok, A. Sentenac, *J. Biol. Chem.* **1997**, *272*, 27980.
[31] M. Blind, W. Kolanus, M. Famulok, *Proc. Natl. Acad. Sci. USA* **1999**, *96*, 3606.
[32] H. Shi, B. E. Hoffman, J. T. Lis, *Proc. Natl. Acad. Sci. USA* **1999**, *96*, 10 033.
[33] G. Mayer, M. Blind, W. Nagel, T. Böhm, T. Knorr, C. L. Jackson, W. Kolanus, M. Famulok, *Proc. Natl. Acad. Sci. USA* **2001**, *98*, 4961.
[34] S. Weiss, D. Proske, M. Neumann, M. H. Groschup, H. A. Kretzschmar, M. Famulok, E. L. Winnacker, *J. Virol.* **1997**, *71*, 8790.
[35] D. Peretz, R. A. Williamson, Y. Matsunaga, H. Serban, C. Pinilla, R. B. Bastidas, R. Rozenshteyn, T. L. James, R. A. Houghten, F. E. Cohen, S. B. Prusiner, D. R. Burton, *J. Mol. Biol.* **1997**, *273*, 614.
[36] S. Supattapone, P. Bosque, T. Muramoto, H. Wille, C. Aagaard, D. Peretz, H. O. Nguyen, C. Heinrich, M. Torchia, J. Safar, F. E. Cohen, S. J. DeArmond, S. B. Prusiner, M. Scott, *Cell* **1999**, *96*, 869.
[37] M. Gasset, M. A. Baldwin, D. Lloyd, J. M. Gabriel, D. M. Holtzmann, F. Cohen, R. J. Fletterick, S. B. Prusiner, *Proc. Natl. Acad. Sci. USA* **1992**, *89*, 10 940.
[38] R. Riek, S. Hornemann, G. Wider, M. Billeter, R. Glockshuber, K. Wüthrich, *Nature* **1996**, *382*, 180.
[39] R. Riek, S. Hornemann, G. Wider, R. Glockshuber, K. Wüthrich, *FEBS Lett.* **1997**, *413*, 282.
[40] R. Zahn, A. Liu, T. Luhrs, R. Riek, C. von Schroetter, F. Lopez Garcia, M. Billeter, L. Calzolai, G. Wider, K. Wüthrich, *Proc. Natl. Acad. Sci. USA* **2000**, *97*, 145.
[41] D. G. Donne, J. H. Viles, D. Groth, I. Mehlhorn, T. L. James, F. E. Cohen, S. B. Prusiner, P. E. Wright, H. J. Dyson, *Proc. Natl. Acad. Sci. USA* **1997**, *94*, 13 452.
[42] H. Zhang, J. Stockel, I. Mehlhorn, D. Groth, M. A. Baldwin, S. B. Prusiner, T. L. James, F. E. Cohen, *Biochemistry* **1997**, *36*, 3543.
[43] F. Lopez Garcia, R. Zahn, R. Riek, K. Wüthrich, *Proc. Natl. Acad. Sci. USA* **2000**, *97*, 8334.
[44] S.-W. Lee, B. A. Sullenger, *Nat. Biotechnol.* **1997**, *15*, 41.
[45] N. C. Pagratis, C. Bell, Y.-F. Chang, S. Jennings, T. Fitzwater, D. Jellinek, C. Dang, *Nat. Biotechnol.* **1997**, *15*, 68.
[46] D. H. Mathews, J. Sabina, M. Zuker, D. H. Turner, *J. Mol. Biol.* **1999**, *288*, 911.
[47] H. M. Schätzl, M. Da Costa, L. Taylor, F. E. Cohen, S. B. Prusiner, *J. Mol. Biol.* **1995**, *245*, 362.
[48] M. R. Scott, R. Kohler, D. Foster, S. B. Prusiner, *Protein Sci.* **1992**, *1*, 986.
[49] W. Xu, A. D. Ellington, *Proc. Natl. Acad. Sci. USA* **1996**, *93*, 7475.
[50] S. J. DeArmond, S. B. Prusiner, *J. Neurochem.* **1993**, *61*, 1589.
[51] A. D. Snow, T. N. Wight, D. Nochlin, Y. Koike, K. Kimata, S. J. DeArmond, S. B. Prusiner, *Lab. Invest.* **1990**, *63*, 601.

[52] A. D. Snow, R. Kisilevsky, J. Willmer, S. B. Prusiner, S. J. DeArmond, *Acta Neuropathol.* **1989**, *77*, 337.
[53] M. E. Bruce, P. A. McBride, C. F. Farquhar, *Neurosci. Lett.* **1989**, *102*, 1.
[54] B. Caughey, G. J. Raymond, *J. Virol.* **1993**, *67*, 643.
[55] K. Doh-Ura, T. Iwaki, B. Caughey, *J. Virol.* **2000**, *74*, 4894.
[56] D. P. C. McGee, A. VaughnSettle, C. Vargeese, Y. S. Zhai, *J. Org. Chem.* **1996**, *61*, 781.
[57] J. Ludwig, F. Eckstein, *J. Org. Chem.* **1989**, *54*, 631.
[58] D. Jellinek, L. S. Green, C. Bell, N. Janjic, *Biochemistry* **1994**, *33*, 10450.
[59] A. Taraboulos, A. J. Raeber, D. R. Borchelt, D. Serban, S. B. Prusiner, *Mol. Biol. Cell.* **1992**, *3*, 851.

Received: February 6, 2002
Revised version: May 5, 2002 [F 356]